THE USE OF SURFACE ACOUSTIC WAVES TO STUDY SMALL FATIGUE CRACKS IN 7075-T651 ALUMINUM AND 4340 STEEL

H.H. Yuce†, D.V. Nelson† and M.T. Resch††

† Department of Mechanical Engineering
††Department of Materials Science and Engineering
Stanford University
Stanford, California 94305

INTRODUCTION

SAW-NDE techniques make it possible to utilize interactions between acoustic waves and small surface cracks to obtain important information about fatigue behavior during crack growth measurements, such as crack depth and opening behavior below the surface.

Progress has been made in refinement of a theoretical model for determining microcrack depth based on optical measurements of crack length on the surface and SAW measurement of crack reflection coefficients. In particular, the scattering model of Resch et al[1-4] has demonstrated the ability of the SAW technique to obtain microcrack depth in Pyrex glass and 7075-T6 aluminum specimens. In the results reported here, the SAW technique, with the improved scattering model, was used to determine crack depth in quenched and tempered 4340 steel specimens. In addition, measurements of the reflection coefficient from a microcrack in a 7075-T6 specimen showed that the crack opening behavior can be monitored during a fatigue experiment. Comparisons of acoustically determined opening behavior with that obtained from scanning electron microscope measurements of crack mouth opening displacement (CMOD) show that SAW techniques can reveal changes in opening behavior below the surface that are not detected by conventional techniques which rely only on information at the surface. Changes in opening stress with crack growth are reported.

IMPROVEMENTS IN ACOUSTIC THEORY

Scattering Model of Resch et al.

Kino[5] and Auld[6] have developed a general scattering theory which describes the relative wave amplitude scattered from one transducer to another by a void of arbitrary shape. They have shown that the reflection coefficient of a Rayleigh wave normally incident on a small surface crack growing normal to the surface can be written as:

$$S_{21} = \frac{A_r}{A_i} = \frac{j\omega}{2P} \psi^R \qquad (1)$$

where A_r is the amplitude of the reflected signal from the crack, A_i is the amplitude of the incident signal, P is the input power to the transmitting transducer, ω is the frequency of the Rayleigh wave, $j = \sqrt{-1}$, and ψ^R is the elastic energy released by a surface crack in the stress field of a surface acoustic wave, which can be written as [4]:

$$\psi^R = \frac{1-\nu^2}{3E} \int_S \rho K_I^2 ds \qquad (2)$$

where ν is Poisson's ratio, E is the modulus of elasticity, ρ is the shortest distance between the origin and tangent line at a given point s as shown in Fig. 1, K_I is the mode I stress intensity factor, and S is the line around the crack edge. For the case of a surface crack in a finite plate subjected to pure bending, Smith et al.[7] have numerically evaluated the stress intensity factor around the edge of a half-penny shaped crack for $\nu = 1/3$. Tien et al.[8] showed that these results can be used to calculate approximately the perturbed stress fields at a half-penny shaped surface crack experiencing the stresses due to a Rayleigh wave, under the limitation that $ka < 1$, where $k = 2\pi/\lambda$ = wave number of the SAW (λ = wavelength) and a is the maximum crack depth. Using Tien's results, Resch et al.[1-4] have shown that the maximum crack depth, a, of a surface crack can be evaluated by acoustically measuring the SAW reflection coefficient from a crack and optically measuring its surface length, 2c.

Improved Model

In order to calculate the reflection coefficient, S_{21}, as defined in Eqn. 1, the distribution of stress intensity factor around the crack edge is needed. The improved model uses the mode I stress intensity factor results for semi-elliptical surface cracks in a plate in pure bending from Newman and Raju[9], valid for variable crack aspect ratio, a/c, between zero and unity and for ν equal to 0.3. This is more appropriate for evaluation of experimental studies using steel samples. The use of Newman and Raju's results accounts for the effects of ellipticity of the crack shape as well as of the non-uniform stress field of a SAW on the magnitude of the reflection coefficient from a crack. As seen in Eqn. 2, to evaluate the elastic energy released by a surface crack in the stress field of surface acoustic wave, a numerical integration of stress intensity factor around the crack edge was needed in the new model. Reflection coefficient versus normalized crack depth for a half-penny shaped surface crack using the two models is given in Fig. 2. (The half-penny shape was selected for comparison purposes. The new model can handle variable crack aspect ratio, a/c.) The solid line in this figure shows the results of the model of Resch et al. for $\nu = 1/3$ and the dashed line shows the results of the improved model for $\nu = 0.30$. Up to ka of about 0.6, results from both models are close but as ka becomes larger, the difference increases, to about 25% at $ka \simeq 1.0$.

The results of acoustically predicted crack depth versus post fracture measured depth, utilizing the new model, are shown in Fig. 3. Excellent acoustic predictions of crack depth in quenched and tempered 4340 steel are obtained.

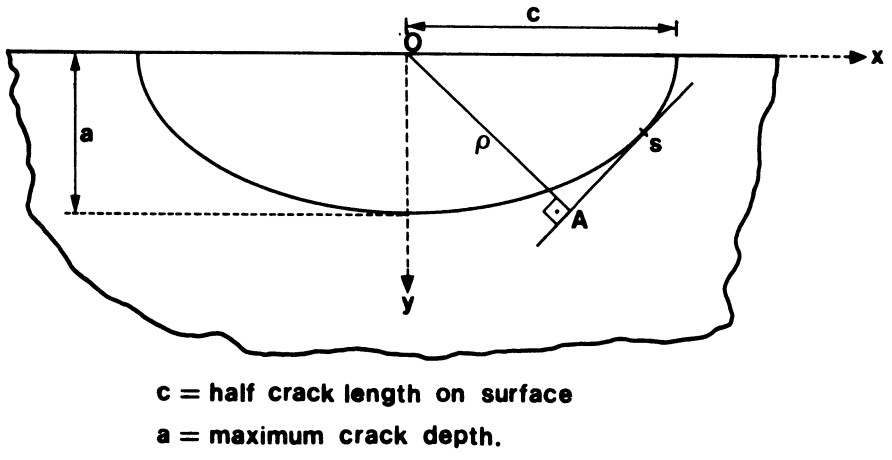

Figure 1. Schematic of semi-elliptical surface crack.

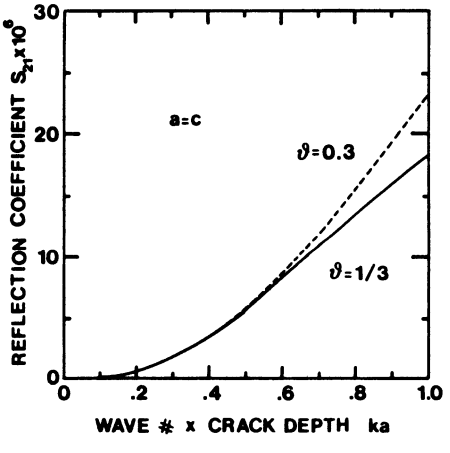

Figure 2. Reflection coefficient versus normalized crack depth.

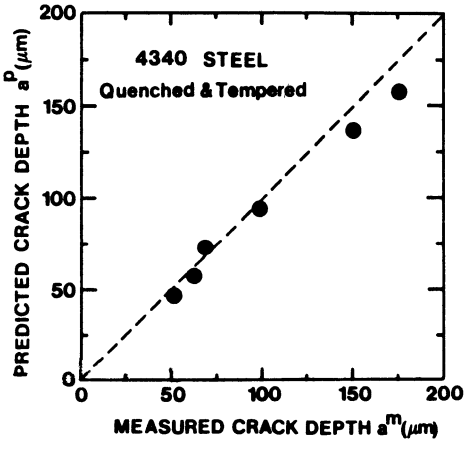

Figure 3. Acoustically predicted crack depth versus measured post-fracture crack depth.

STUDYING SHORT CRACK GROWTH BEHAVIOR BY USING A SAW/SEM TECHNIQUE

Morris et al.[10-11] have demonstrated the feasibility of crack mouth opening displacement (CMOD) and crack tip opening displacement (CTOD) measurements in a SEM for determining the opening behavior of small surface cracks. The procedure is to make measurements of CMOD and CTOD for a specimen containing a microcrack while it is under static load in the vacuum chamber of an SEM. Opening stress is taken as the point where the slope of CMOD (or CTOD) versus stress changes markedly, as depicted in Fig. 4. It is important to know the opening stress since the effective stress range driving crack growth is the difference between the maximum applied stress and opening stress.

We are conducting a set of experiments to investigate the relationship between the optically determined crack opening stress, σ_{op}, and the stress at which saturation of the SAW reflection coefficient occurs, σ_{sat}. Saturation stress is that value of stress at which the reflection coefficient reaches a constant maximum value, corresponding to a crack fully open in depth. See Fig. 5. The fatigue specimen and cantilevered flexure jig used for CMOD measurements in an SEM are shown in Fig. 6. Specimens are prepared for combined SAW/SEM testing as follows:

- o Start with a specimen of 6 mm thickness.
- o Pin point laser burn it to initiate a damage zone in the area we want to crack.
- o Conduct fatigue crack initiation and growth testing until a crack size of $\simeq$ 100 μm to 200 μm surface length is obtained.
- o Shave the surface until a minimum detectable crack size with the SAW technique is obtained.
- o Bring the specimen thickness to 5 mm by removing material from the side opposite the crack.
- o Attach a strain-gage on the opposite side of the specimen to measure the stress throughout the fatigue test and during loading in the SEM jig.

Measurements of SAW reflection coefficient are made in a fatigue testing machine with the specimen in cantilevered bending by adjusting the specimen deflection to give the desired strain levels. After fatigue cycling and the acoustic measurements are completed, the specimen is then removed from the testing machine, mounted on the small flexure jig shown in Fig. 6, and placed in the chamber of an SEM. For the particular value of stress (strain) being studied, the CMOD is then measured at a magnification of approximately 50,000 X. Then the specimen is returned for additional fatigue cycling and the measurements repeated. Recent complete results from one of these specimens, made of 7075-T651 aluminum, are given in Figs. 4 and 5. In this experiment, changes in opening behavior of a small surface crack are evaluated at intervals of: N=0, 19,950, 28,650, 37,100, 53,180, and 84,500 cycles for a fully reversed constant stress amplitude of $\pm$ 75% of the cyclic yield stress, or approximately 375 MPa.

Fig. 7 shows changes in the saturation stress and in the opening stress determined by CMOD measurements during the course of fatigue testing. Fig. 8 shows the change in the crack aspect ratio, a/c, with number of fatigue cycles. The SAW technique is able to monitor how the crack aspect ratio varies with growth, knowledge of which is very important in calculating stress intensity factor or other parameters which may be used to try to correlate crack growth behavior. Such information cannot, of course, be obtained only from surface

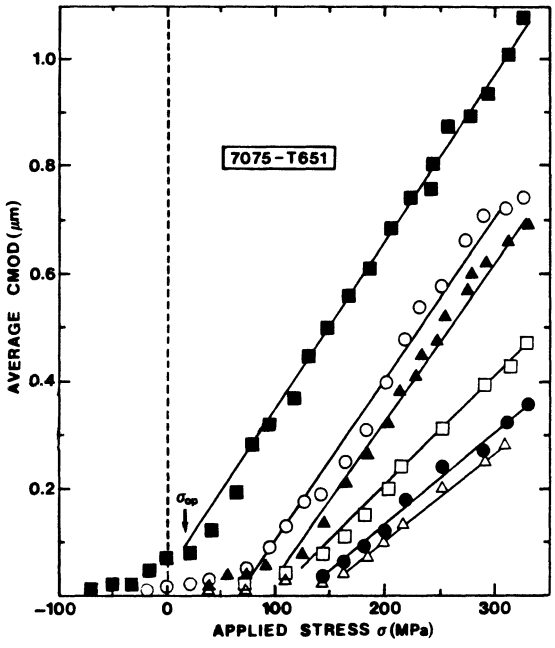

Figure 4. CMOD versus applied stress.

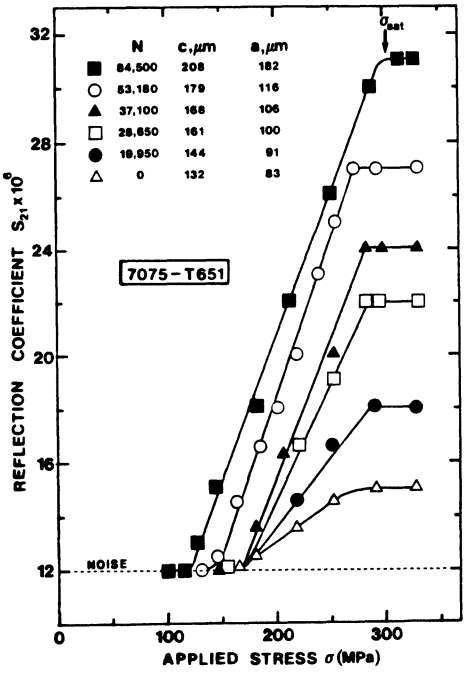

Figure 5. Reflection coefficient vs. applied stress.

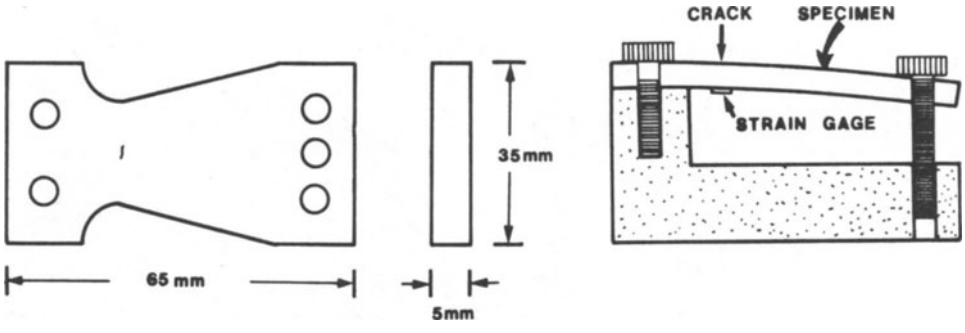

Figure 6. Schematic of fatigue sample and SEM jig.

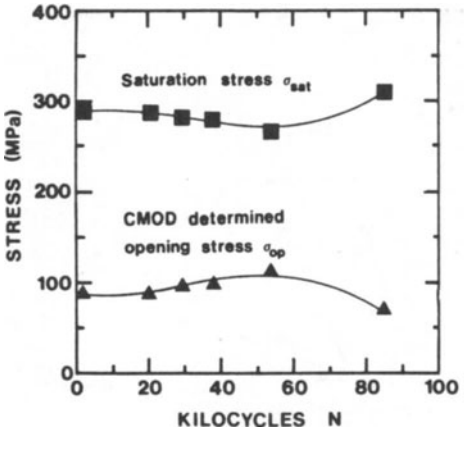

Figure 7. Saturation stress and opening stress versus number of fatigue cycles.

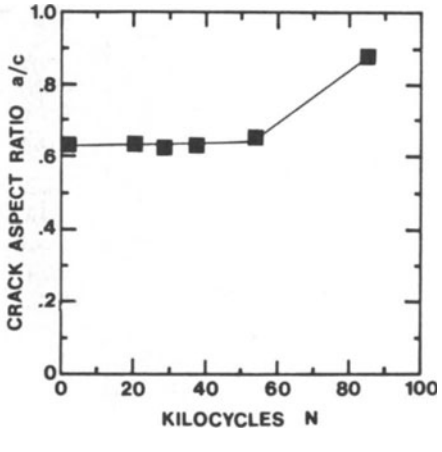

Figure 8. Crack aspect ratio versus number of fatigue cycles.

measurements. Fig. 9 shows the complete map of crack opening behavior with number of fatigue cycles. In this figure the change in saturation stress, σ_{sat}, and opening stress, σ_{op}, during the test are shown. During the experiment when the applied stress is equal to σ_{op}, the crack is starting to open on the surface and when it is equal to σ_{sat}, the crack is fully open. In other words, from σ_{op} to σ_{sat}, it is partially open and above σ_{sat}, up to σ_{max}, it is fully open. Fig. 10 shows the change in mode I stress intensity factor range, ΔK_I, versus number of fatigue cycles. Here, stress intensity factor is calculated based on the applied stress range using Newman and Raju's stress intensity factor solutions for surface cracks under bending. The line with triangles shows the change in ΔK_I at the maximum crack depth and the line with squares shows the change in ΔK_I at the surface. Although ΔK_I at the maximum depth was higher than ΔK_I at the surface for most the cycles, as seen in Fig. 10, a crossover occurred as crack aspect ratio, a/c, increased.

Morris and Buck[10-11] defined effective stress range as:

$$\Delta\sigma_{eff_1} = \sigma_{max} - \sigma_{op} \tag{3}$$

Acoustically measured saturation stress, σ_{sat}, shows the applied stress at which crack faces are fully separated. Then one can also propose an effective stress range as:

$$\Delta\sigma_{eff_2} = \sigma_{max} - \sigma_{sat} \tag{4}$$

In Fig. 11, the line with squares shows $\Delta\sigma_{eff1}$ versus number of fatigue cycles and the line with triangles $\Delta\sigma_{eff2}$. Based on these effective stress ranges, one can calculate effective stress intensity factor ranges. As indicated in Fig. 12, the use of ΔK_{eff} based on Eqn. 4 may not be a useful concept for correlating crack growth rate. In any case, these preliminary results show that SAW measurement of opening behavior reveals information about small surface fatigue crack growth that is not detected by more conventional techniques.

Residual Stresses

It is known that the state of residual stress in a test specimen can significantly affect the growth behavior of microcracks. The preliminary experiments were done to check the SAW/SEM technique. Experiments now underway are monitoring surface residual stresses by X-ray diffraction in order to provide additional information to help interpret crack behavior.

CONCLUSIONS

1. An improved acoustic model provided excellent predictions of microcrack depth in 4340 steel.
2. A combined SAW/SEM technique was able to monitor:
   (a) Changes in crack aspect ratio, a/c, during growth,
   (b) Changes in effective stress intensity factor range, ΔK_{eff}, in depth and at the surface, and
   (c) When the crack is fully open in depth.

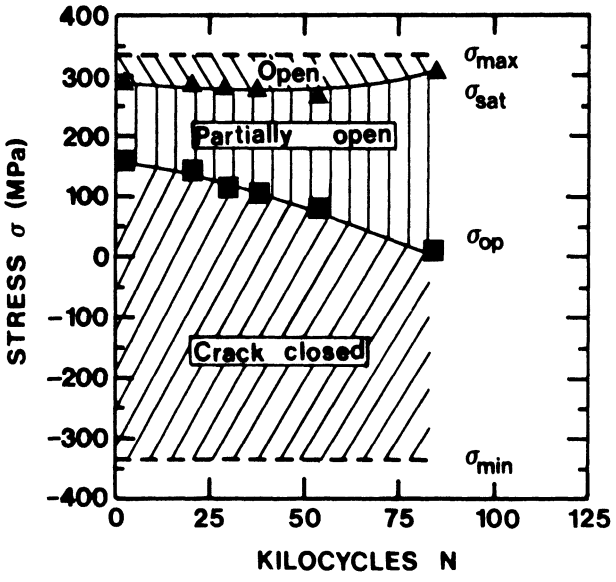

Figure 9. Crack opening behavior versus number of fatigue cycles.

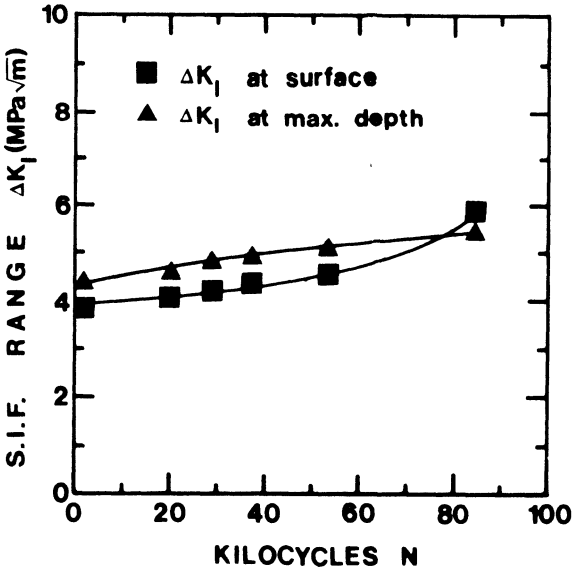

Figure 10. Change in stress intensity factor range with number of fatigue cycles.

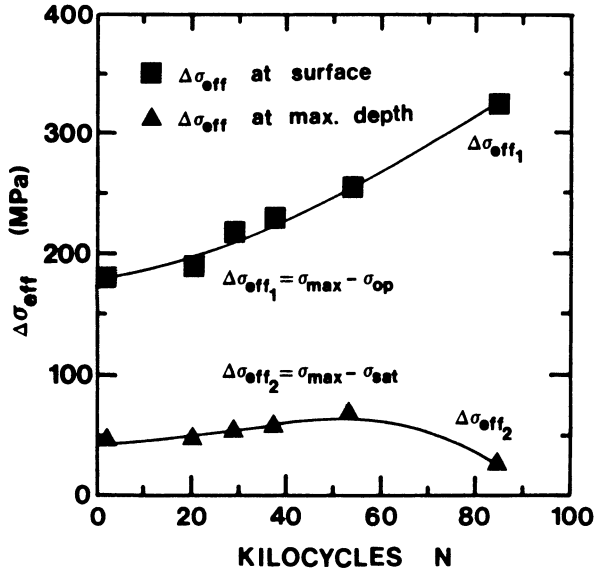

Figure 11. Change in effective stress range with number of fatigue cycles.

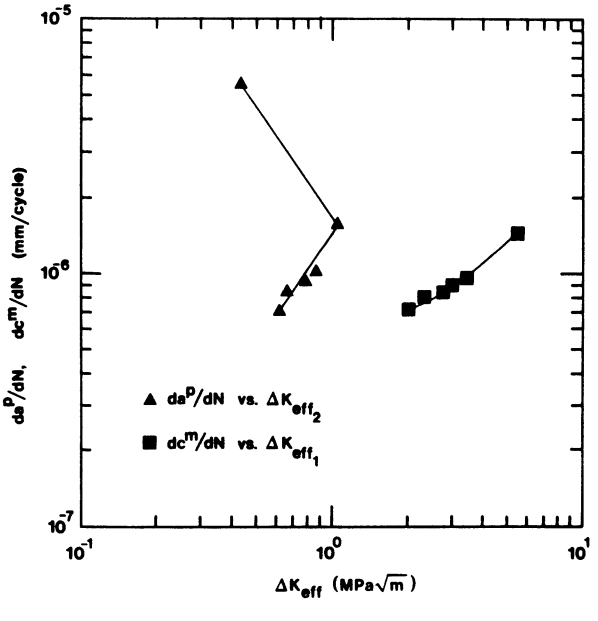

Figure 12. Crack growth rate versus effective stress intensity factor range.

FUTURE WORK

We plan to study:

(a) Small crack growth behavior in 300-M and 4140 steels,
(b) The effects of surface residual stresses on crack growth,
(c) The interaction of small crack growth with microstructural features such as inclusions and prior austenite grain boundaries, at different applied stress amplitudes and mean stress levels,
(d) The influences of different microstructures in 4140 steel on small crack growth.

ACKNOWLEDGEMENT

The authors wish to thank the United States Department of Energy, Office of Basic Energy Sciences, Division of Materials Sciences (Dr. S. Wolf) for supporting this research.

REFERENCES

1. M. T. Resch, B. D. London, G. F.Ramusat, H. H. Yuce, D. V. Nelson and J.C. Shyne, "SAW NDE Techniques for Monitoring the Growth Behavior of Small Surface Fatigue Cracks", Review of Progress in Quantitative Non-destructive Evaluation, D. O. Thompson and D. E. Chimenti, eds., Plenum Press, New York, Vol. 3A, pp. 217-227 (1984).

2. M. T. Resch, J. C. Shyne, G. S. Kino and D. V. Nelson, "Long Wavelength Rayleigh Wave Scattering from Microscopic Surface Fatigue Cracks", Proc. ARPA/AFML Review of Progress in Quantitative NDE, D. O. Thompson and D. E. Chimenti, eds., Plenum Press, New York, Vol. 1, pp. 573-578 (1982).

3. M. T. Resch, D. V. Nelson, J. C. Shyne and G. S. Kino, "Acoustic Monitoring of Small Surface Fatigue Crack Growth", Advances in Crack Length Measurement, C. J. Beevers, ed., Engineering Materials Advisory Services, Ltd., West Midlands, England, pp. 473-504 (1982).

4. M. T. Resch, "Non-Destructive Evaluation of Small Surface Cracks Using Surface Acoustic Waves", Doctoral Dissertation, Stanford University, Stanford, California (1982).

5. G. S. Kino, "The Application of Reciprocity Theory to Scattering of Acoustic Waves by Flaws", J. Appl. Phys., Vol. 49, No. 6, pp. 3190-3190 (1978).

6. B. A. Auld, "General Electro-mechanical Reciprocity Relations Applied to the Calculations of Elastic Wave Scattering Coefficients", Wave Motion, Vol. 1, No. 1, pp. 3-10 (1979).

7. F. W. Smith, A. F. Emery and A. S. Kobayashi, "Stress Intensity Factor for Semicircular Cracks, Part II Semi-Infinite Solids", J. Appl. Mechs., Vol. 34, No. 83. pp. 953-959 (December, 1967).

8. J. Tien, B. Khuri-Yakub and G. S. Kino, "Acoustic Surface Wave Probing of Ceramics", Report #AFWAL-TR-80-4078, Proceedings of the DARPA/AFML Review of Progress in Quantitative Non-destructive Evaluation, La Jolla, California, pp. 671-677 (1980).

9. J. C. Newman, Jr., I. S. Raju, "Analysis of Surface Cracks in Finite Plates Under Tension or Bending Loads", NASA Technical Paper No. 1578 (1979).

10. W. L. Morris, "The Non-Continuum Crack Tip Deformation Behavior of Surface Microcracks", Met. Trans., Vol. 11A, pp. 1117-1123 (1980).

11. W. L. Morris, M. R. James and O. Buck, "Growth Rate Models for Short Surface Cracks in Al 2219-T851", Met. Trans., Vol. 12A, pp. 57-69 (1981).